Nuclear isovector valence-shell excitation of ^{202}Hg

R. Kern, R. Stegmann, N. Pietralla, G. Rainovski, M. P. Carpenter, R. V. F. Janssens, M. Lettmann, O. Möller, T. Möller, C. Stahl, V. Werner, and S. Zhu

Phys. Rev. C **99**, 011303 — Published 9 January 2019

DOI: 10.1103/PhysRevC.99.011303

Nuclear Isovector Valence-Shell Excitation of ^{202}Hg

R. Kern[1],* R. Stegmann[1], N. Pietralla[1], G. Rainovski[2], M. P. Carpenter[3], R. V. F. Janssens[4,5], M. Lettmann[1], T. Möller[1], O. Möller[1], C. Stahl[1], V. Werner[1], and S. Zhu[3]

[1] *Institut für Kernphysik, Technische Universität Darmstadt, 64283 Darmstadt, Germany*
[2] *Faculty of Physics, University of Sofia St. Kliment Ohridski, 1164 Sofia, Bulgaria*
[3] *Physics Division, Argonne National Laboratory, Argonne, Illinois 60439, USA*
[4] *Department of Physics and Astronomy, University of North Carolina at Chapel Hill, Chapel Hill, North Carolina 27559, USA and*
[5] *Triangle Universities Nuclear Labratory, Duke University, Dunham, North Carolina 27708, USA*

(Dated: December 6, 2018)

Excited states of ^{202}Hg have been studied via the ^{12}C(^{202}Hg,^{202}Hg*) Coulomb excitation reaction at a beam energy of 890 MeV. The γ-ray transitions from the excited states of ^{202}Hg were detected by the Gammasphere array. The intensities of the observed γ rays determined the relative populations of the excited states which were used to extract the absolute $M1$ and $E2$ transition strength distributions for excited 2^+ states of ^{202}Hg up to 2 MeV. The measured absolute $B(M1; 2^+_7 \to 2^+_1)$ strength of $0.18\,(8)\,\mu_{\mathrm{N}}{}^2$ indicates that the 2^+_7 level of ^{202}Hg is the main fragment of the proton-neutron mixed-symmetry $2^+_{1,\mathrm{ms}}$ state. Upper limits for the F-spin mixing matrix elements of ^{202,204}Hg are determined as well.

The emergence of nuclear collectivity from the effective nucleon-nucleon interactions represents one of the outstanding challenges in nuclear structure physics. One of these effective interactions is the attractive quadrupole-quadrupole interaction between valence protons and neutrons. It is known to be the reason for quadrupole collectivity in most heavy, open-shell nuclei. It leads to a coherent mixing of collective quadrupole excitations of the proton and neutron sub-spaces and, thus, to low-energy nuclear states in which protons and neutrons collectively move in phase. This collective mode can successfully be described by geometrical models which consider the nucleus as a homogeneous object with a certain shape which can vibrate or rotate [1]. The main disadvantage of this approach is the complete loss of the fundamental many-body character of the nuclear system.

A theoretical approach to the modeling of quadrupole-collective heavy nuclei which provides an attempt to bridge the calculation of nuclear properties from fundamental nucleon-nucleon interactions to the collective model is the Interacting Boson Model [2]. Its sd-IBM-2 version [3, 4], which describes the quadrupole-collective excitations in even-even nuclei, uses the approximation that valence nucleons are pairwise coupled to N_π proton or N_ν neutron monopole (s) or quadrupole (d) bosons. In a panoply of case studies, the IBM has been demonstrated [4] to successfully describe the main features of quadrupole-collective nuclear structures and the shape transitions between them as a function of valence nucleon numbers. The sd-IBM-2 yields quantum states that are characterized by a certain degree of coherence of proton-boson and neutron-boson contributions. This coherence is quantified by the F-spin which is, for valence bosons, the analogue to isospin for nucleons. The lowest-lying states are characterized by the F-spin quantum number $\mathrm{F} = \mathrm{F}_{\mathrm{max}} = (\mathrm{N}_\pi + \mathrm{N}_\nu)/2$ and their boson wave functions are completely symmetric under pairwise exchange of proton and neutron bosons.

Besides these full-symmetry states (FSS), the sd-IBM-2 predicts, in addition, the existence of an entire class of states with wave functions that contain parts that are antisymmetric under the pairwise exchange of proton and neutron bosons [3]. These mixed-symmetry states (MSS) are characterized by F-spin quantum numbers $\mathrm{F} \leq \mathrm{F}_{\mathrm{max}} - 1$. Their properties, such as excitation energy, electromagnetic decay or F-spin purity, are sensitive to some parameters of the sd-IBM-2 space that are not accessible otherwise, such as the strength of the Majorana interaction, F-vector boson transition charges, or the size of the mixing matrix element between FSS and MSS.

According to the IBM-2, the lowest-lying isovector valence-shell excitation in vibrational nuclei is the one-quadrupole-phonon $2^+_{1,\mathrm{ms}}$ state [3, 4]. The isovector character leads to unique decay properties of this $2^+_{1,\mathrm{ms}}$ state. The most indicative signature is a strong $M1$ transition to the fully-symmetric one-quadrupole-phonon 2^+_1 state, as well as a weakly-collective $E2$ transition (≈ 1 W.u.) to the ground state [5–9]. This strong $M1$ matrix element ($|\langle 2^+_1||M1||2^+_{1,\mathrm{ms}}\rangle| \approx 1\,\mu_{\mathrm{N}}$) [9], which is forbidden for isoscalar transitions [10], serves as the main experimental signature used for identification of one-phonon MSSs. A further signature is an enhanced E1 transition between the full-symmetry octupole state and the $2^+_{1,\mathrm{ms}}$ state in comparison to the 2^+_1 state [9]. This is due to the isovector nature of the $E1$ transition operator in the same manner as the isovector nature of the $M1$ transition operator enhances the $M1$ transition strengths between MSSs and FSSs [11].

One-quadrupole-phonon MSSs were identified all across the nuclear chart; in the mass $A \approx 90$ region [6, 12, 13], as well in the mass $A \approx 130$ region [14–19] and, most recently, in the mass $A \approx 200$ region [20, 21]. The experimental information accumulated up to now suggests that pronounced one-phonon MSSs can

* rkern@ikp.tu-darmstadt.de

be expected when both protons and neutrons occupy orbitals with high angular momenta as in the case of ^{212}Po [20]. However, ^{204}Hg offers an opposite example - even though its valence structure is dominated by orbitals with small angular momenta for both protons and neutrons, ^{204}Hg exhibits a $2^+_{1,\mathrm{ms}}$ state with an even larger $M1$ decay strength than in ^{212}Po [20, 21]. ^{202}Hg exhibits a similar valence structure as ^{204}Hg, but with two additional neutron holes. Low-lying states of ^{202}Hg can be formed from excitations of the valence holes to the $\pi(2d_{3/2})^{-2}\,\nu(2f_{5/2})^{-2}(3p_{3/2})^{-2}$ orbitals. Its structure is dominated by orbitals with small angular momenta similar to the structure of ^{204}Hg. The extent to which a model space of several low-spin orbitals is capable of supporting F-spin symmetry is unknown as more bosons contribute to the wave functions.

This experiment aims to identify the $2^+_{1,\mathrm{ms}}$ state of ^{202}Hg and to determine how its properties change in comparison to the known $2^+_{1,\mathrm{ms}}$ states of isotopes in the vicinity of the doubly-magic nucleus ^{208}Pb, especially ^{204}Hg. Furthermore, it is intriguing to analyze and compare the evolution of F-spin mixing of $Z = 80$ isotopes to the one observed in $N = 80$ isotones. Hence, a projectile Coulomb excitation measurement was carried out to populate 2^+ states and to search for the one-quadrupole-phonon MSS of ^{202}Hg.

The experiment was performed with a beam of stable ^{202}Hg ions at the ATLAS facility at Argonne National Laboratory. The pulsed (12 MHz) beam was accelerated up to 890 MeV and impinged on a 1 mg/cm^2-thick $^{\mathrm{nat}}$C target. The target chamber was surrounded by Gammasphere [22], which for this experiment was composed of 100 HPGe detectors arranged in 16 rings. Data were recorded when one γ ray was detected in any HPGe detector. The chosen beam energy is equivalent to $\approx$ 85 % of the Coulomb barrier for the ^{202}Hg + ^{12}C reaction. A total of 8.4×10^8 events of γ-ray fold ≥ 1 was collected over a period of 20 h. To suppress the background, the "beam-off" (with respect to the accelerator radio frequency) spectrum was subtracted from the "beam-on" spectrum, appropriately scaled to minimize the 1461-keV ^{40}K room background transition. The Doppler-corrected, background-subtracted singles spectrum of this high statistics measurement is dominated by the 439-keV, $2^+_1 \rightarrow 0^+_1$ transition in ^{202}Hg, with 2.5×10^8 events (see Fig. 1 a). About 2% of the data consists of γ-ray coincidence events of fold 2 or higher and was sorted in an E$_\gamma$-E$_\gamma$ matrix. A spectrum of γ rays in coincidence with the $2^+_1 \rightarrow 0^+_1$ transition is provided in Fig. 1 b. In the present experiment, 39 peaks have been observed which can be firmly assigned to transitions between excited levels of ^{202}Hg [23–33]. The resulting level scheme is shown in Fig. 2. Spin and parity quantum numbers were adopted from Ref. [34]. In the present reaction, eight 2^+ states of ^{202}Hg were populated. The lowest-lying 2^+ level at 439 keV is the fully-symmetric one-quadrupole-phonon excitation. Concerning the assignment of the $2^+_{1,\mathrm{ms}}$ state with the decay signature described above, the 2^+ level at 1794 keV appears to be the most promising candidate as

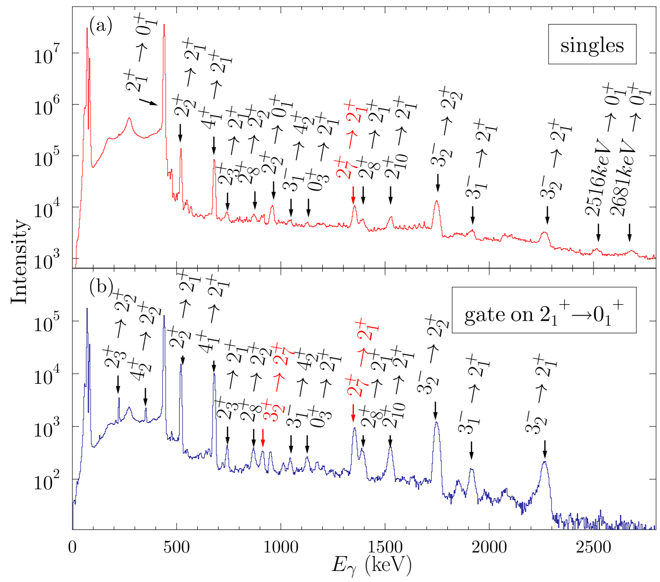

FIG. 1. (color online). Doppler-corrected, time-background subtracted γ-ray spectra after projectile Coulomb excitation on a $^{\mathrm{nat}}$C target; (a) singles spectrum; (b) spectrum of γ rays in coincidence with the $2^+_1 \rightarrow 0^+_1$ transition. In both spectra the transitions relevant for this study are highlighted.

the main fragment. In the region of $\approx$ 2 MeV excitation, where the $2^+_{1,\mathrm{ms}}$ level is expected, it is the state populated with the highest intensity. It decays predominantly via the 1354-keV transition to the 2^+_1 state with an additional small branch to the 2^+_2 state via the 833-keV γ ray. The 2^+ state at 1823 keV exhibits a similar decay pattern and appears to be a small fragment of the $2^+_{1,\mathrm{ms}}$ state. The intensity of its strongest decay, via the 1384-keV transition, to the 2^+_1 state is only one fifth that of the 1354-keV transition of the 1794-keV level. Negative-parity states of ^{202}Hg have also been populated in the present measurement. Three 3^- levels were observed at 2357, 2709 and 3166 keV, with the largest feeding reaching the second state. Besides the 3^- states, one further negative-parity state, a 5^- state at 1966 keV, was populated. In addition to the 2^+ and negative-parity levels, two 4^+ states were observed at 1120 and 1312 keV, two 0^+ levels at 1564 and 1643 keV, as well as a single 6^+ level at 1989 keV. Finally, it is worth noting that six additional levels with unknown spin and parity quantum numbers are also present in our data with respective energies of 1348, 2134, 2293, 2456, 2516 and 2681 keV. Only the 2681-keV state has not been observed in earlier work [34]. Table I reports on the properties of the levels seen in the present work.

The Coulomb-excitation yields for the populated ^{202}Hg levels are determined through the intensities of the observed γ rays, complemented with known branching ratios, and calculated electron-conversion coefficients [35]. The yields of excited levels relative to that of the 2^+_1 state measure their Coulomb excitation cross section relative to the 2^+_1 state. The experimental relative yields were fitted to the Winther-de Boer theory [36] using the mul-

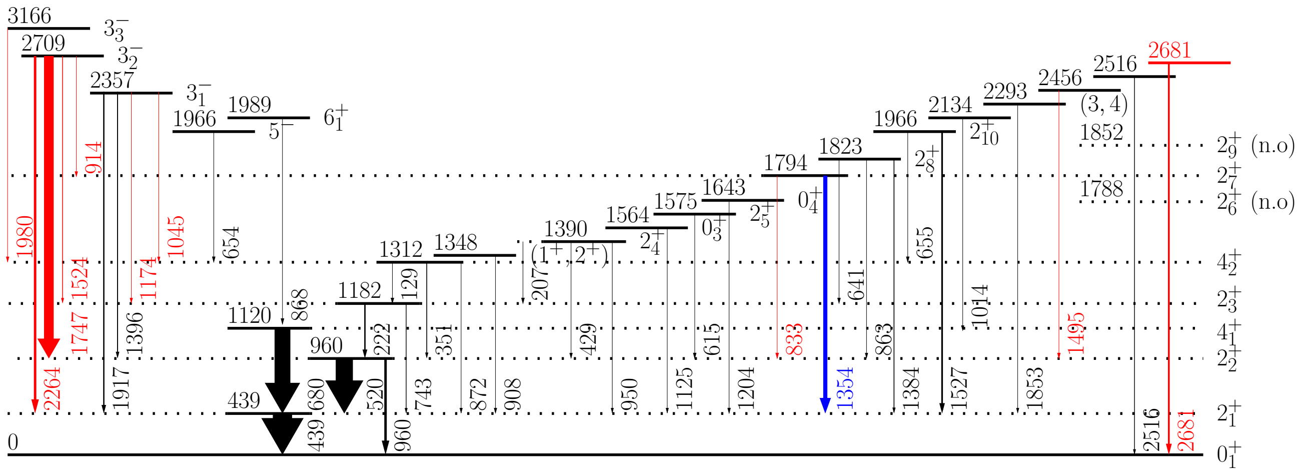

FIG. 2. (color online). Experimental level scheme of ^{202}Hg from this work. The thickness of the arrows corresponds to the intensities measured in the present work. The $2_1^+ \to 0^+$ transition intensity is scaled down to fit into the figure. Newly observed transitions and levels are highlighted (red). The transition $2_7^+ \to 2_1^+$ is also highlighted (blue) as the 2_7^+ state is proposed to correspond to the dominant fragment of the $2_{1,\mathrm{ms}}^+$ state.

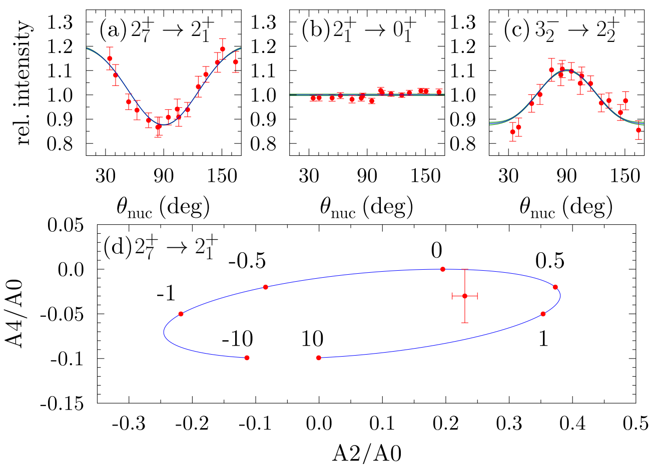

FIG. 3. (color online). Angular distributions measured for the 1354- (a), 439- (b) and 1747-keV (c) transitions. The solid line are fits, in (a) and (c) to a sum of Legendre polynomials, and in (b) to a constant. The resulting A_2/A_0 and A_4/A_0 coefficients of the 1354-keV transition are compared to an angular distribution ellipse (d) calculated with the statistical tensor for the 2_7^+ state. The numbers on the ellipse denote the multipole mixing ratio δ for the $2_7^+ \to 2_1^+$ transition.

tiple Coulomb excitation code CLX [37], while taking the energy loss of the beam in the target into account. Absolute cross sections were derived using the previously measured values for the reduced transition probability; i.e., $B(E2;2_1^+ \to 0_1^+) = 17.35\,(14)$ W.u. [27, 38] and the quadrupole moment $\mathrm{Q}(2_1^+) = 1.01\,(13)\,\mathrm{e}^2\mathrm{b}^2$ [38], providing an unambiguous set of transition matrix elements for one-step excitation. This information in combination with the experimental branching and multipole mixing ratios can be used to obtain the $E2$ and $M1$ strengths distributions for the deexcitation of the excited 2^+ states. The $4\,\pi$ coverage and the resulting high detection efficiency of Gammasphere enable measurements of angular distributions (cf. Fig. 3) for sufficiently intense transitions. This allows to extract the A_2/A_0 and A_4/A_0 coefficients given in Table I. A good example for a γ ray with pronounced anisotropy is the $3_2^- \to 2_2^+$ transition at 1747 keV with its clear dipole character. States with lifetimes of a few tens of picoseconds show flat or attenuated distributions due to the recoil in vacuum effect [39]. This effect causes the isotropy of the $2_1^+ \to 0_1^+$ $[\tau(2_1^+) = 39.3\,(3)\,\mathrm{ps}]$ transition and the attenuation of the angular distribution of the $4_1^+ \to 2_1^+$ $[\tau(4_1^+) = 3.0\,(1)\,\mathrm{ps}]$ and $2_2^+ \to 2_1^+$ $[\tau(2_2^+) = 20\,(4)\,\mathrm{ps}]$ ones. For the $2_3^+ \to 2_2^+$, $2_3^+ \to 2_1^+$ and $2_7^+ \to 2_1^+$ transitions, the extracted angular distribution coefficients are presented in Table I. Wherever possible, the measured angular distributions agree with the previously adopted spin-parity assignments found in Ref. [34]. The multipole mixing ratios of $2^+ \to 2_1^+$ transitions were worked out with an iterative procedure. The technique is described in Ref. [21] and is based on fitting, with the Coulomb excitation code GOSIA [41], transition matrix elements for a subset of states to Coulomb cross sections; e.g., the 2^+ level of interest, the most populated 3^- state, the 2_1^+ level and the ground state. The only free parameter in this procedure is the $E2/M1$ multipole mixing ratio of the $2^+ \to 2_1^+$ transition being considered. The outcome of this method is a decisively small multipole mixing ratio $\delta = 0.06\,(4)$ for the $2_7^+ \to 2_1^+$ transition (cf. Table I and Fig. 3), which indicates its predominant $M1$ character making the assignment of δ from the angular distribution (cf. Fig. 3 d) unique.

This experiment was performed to determine $M1$ strengths of $2^+ \to 2_1^+$ transitions in order to identify the $2_{1,\mathrm{ms}}^+$ state of ^{202}Hg. For the 2_7^+ state at 1794 keV, a transition strength of $B(M1;2_7^+ \to 2_1^+) = 0.18\,(8)\ \mu_{\mathrm{N}}{}^2$ was measured, a value significantly larger than the $10^{-2}\ \mu_{\mathrm{N}}{}^2$ one typically observes between FSSs [9]. This should

TABLE I. Measured properties of the levels and γ-ray transitions in ^{202}Hg. Level energies and spin assignments are adopted from Ref. [34], unless otherwise noted. The relative γ-ray intensities are corrected for efficiency.

E_{Level} (keV)	J^π	E_γ (keV)	J^π_f	I_γ	A_2/A_0	A_4/A_0	δ	$E\lambda$	$B(E\lambda)\downarrow^{ab}$	$B(M1)\downarrow^{b}$	$B(E\lambda)_{\rm lit}$ ^{bc}
439	2^+_1	439	0^+_1	$1.00(1)\cdot 10^6$	0.012(7)	0.002(11)		$E2$			17.35(14) [27, 38]
960	2^+_2	960	0^+_1	620(13)				$E2$	0.039(3)		0.087(21) [27, 28]
		520	2^+_1	4444(44)	0.11(1)	0.012(16)	0.9(1)[40]	$E2$	2.7(3)	$43(8)\cdot 10^{-4}$	5.6(15)[40]
1120	4^+_1	680	2^+_1	4008(41)	0.16(2)	$-0.01(3)$		$E2$	26.6(5)		26.5(8) [27, 28]
1182	2^+_3	1182	0^+_1	< 50 [d]				$E2$	< 0.015		
		743	2^+_1	183(4)	0.21(4)	$-0.039(54)$	2.1(4)	$E2$	$0.54^{+0.09}_{-0.47}$	$33^{+5}_{-29}\cdot 10^{-5}$	
		222	2^+_2	356(15)	0.12(2)	$-0.007(22)$	$-0.13(3)$	$E2$	9^{+5}_{-8}	$0.13^{+0.07}_{-0.12}$	
1312	4^+_2	872	2^+_1	113(13)				$E2$	0.74(6)		
		352	2^+_2	221(9)				$E2$	137(17)		
		129	2^+_3	38(17)				$E2$	3413(1216)		
1348	(2^+) [e]	908	2^+_1	73(7)				$E2$	1.52(4)		
1390	2^+_4	1390	0^+_1	15(6) [d]				$E2$	0.013(1)		
		950	2^+_1	136(6)				$E2$	< 1	$< 6\cdot 10^{-3}$	
		429	2^+_2	39(4)				$E2$	12(4)		
		207	2^+_3	20(5)				$E2$	234(96)		
1564	0^+_3	1125	2^+_1	114(6)				$E2$	5.8(2)		
1575	2^+_5	1136	2^+_1	15(5) [d]				$E2$	0.47(2)		
		615	2^+_2	26(3)				$E2$	17(6)		
1643	0^+_4	1204	2^+_1	44(6)				$E2$	2.6(1)		
1794	2^+_7	1794	0^+_1	30(14) [d]				$E2$	0.13(6)		
		1354	2^+_1	1086(17)	0.23(2)	0.028(25)	0.06(4)	$E2$	0.1(1)	0.18(8)	
		833 [f]	2^+_2	33(7)				$E2$	6(3)		
1823	2^+_8	1823	0^+_1	18(7) [d]				$E2$	0.052(3)		
		1384	2^+_1	221(13)				$E2$	< 4	< 0.027	
		864	2^+_2	91(7)				$E2$	11(4)		
		641	2^+_3	37(3)				$E2$	19(7)		
1966	5^-_1	654	4^+_2	78(5)				$E1$			
1966	2^+_{10}	1527	2^+_1	171(30)				$E2$	10.0(3)		
		655	4^+_2	14(3)				$E2$	55(22)		
1989	6^+_1	868	4^+_1	21(2)				$E2$	24.9(1)		25 [28]
2134	(2^+) [e]	1014	4^+_1	94(6)				$E2$			
2293	$(3,4)$ [g]	1853	2^+_1	117(8)				$E2$	3.40(5)		
2357	3^-_1	2357	0^+_1					$E3$	2.5(1)		
		1917	2^+_1	328(13)				$E1$			
		1396	2^+_2	247(16)				$E1$			
		1174 [f]	2^+_5	100(8)				$E1$			
		1045 [f]	4^+_2	100(9)				$E1$			
2456	(2^+) [e]	1495 [f]	2^+_2	42(15)				$E2$			
2516	$(1,2)$ [e]	2516	0^+_1	181(11)				$E2$	0.11(1)		
2681 [f]	(2^+) [e]	2681 [f]	0^+_1	226(14)				$E2$	0.20(2)		
2709	3^-_2	2709	0^+_1					$E3$	21(1)		< 25[29]
		2264 [f]	2^+_1	611(23)				$E1$			
		1747 [f]	2^+_2	2431(51)	$-0.17(2)$	0.04(3)		$E1$			
		1524 [f]	2^+_3	373(29)				$E1$			
		914 [f]	2^+_7	122(14)				$E1$			
3166	3^-_3	3166	0^+_1					$E3$	1.0(1)		
		1980 [f]	2^+_1	74(36)				$E1$			

[a] Extracted via Coulomb-excitation analysis in the present experiment.
[b] $B(M1)$ values are given in $\mu_N{}^2$, $B(E2)$, $B(E3)$ and $B(E4)$ values are given in W.u.
($1\,\mathrm{W.u.}(E1) = 2.22\,\mathrm{e^2fm^2}$, $1\,\mathrm{W.u.}(E2) = 70.4\,\mathrm{e^2fm^4}$, $1\,\mathrm{W.u.}(E3) = 2.42\times 10^3\,\mathrm{e^2fm^6}$).
[c] The values in this column are the ones given in Ref. [34], converted to single-particle units.
[d] Calculated via literature branching ratio [34].
[e] Assumed 2^+ state in the analysis.
[f] Newly observed.
[g] Assumed 4^+ state in the analysis.

be viewed as a strong indication that the 2^+_7 level is of mixed-symmetric nature. For the close-lying 2^+_8 state, an upper limit $B(M1; 2^+_8 \rightarrow 2^+_1) < 0.027\,\mu_\mathrm{N}{}^2$, could be extracted. This maximum applies to the extreme assumption of a pure $M1$ character for the $2^+_8 \rightarrow 2^+_1$ transition. The $M1$ strength distribution (cf. Fig. 4) supports the notion that the 2^+_7 level at 1794 keV is the main fragment of the $2^+_{1,\mathrm{ms}}$ state of ^{202}Hg, and that the

2_8^+ state represents at most a small fragment of it. The weakly collective ($\sim$ 0.1 W.u.) $E2$ decay of the 2_7^+ level to the ground state is in line with the expected decay behavior of a MSS. The 3_2^- state at 2709 keV is the most strongly populated negative-parity excitation observed. The measured branching ratio of the γ decays of the 3_2^- state allows to determine the $E1$ ratio [42] $R_{E1} = \frac{B(E1;3_2^-\to2_7^+)}{B(E1;3_2^-\to2_1^+)} \approx 3$. The enhancement of the $E1$ transition to the 2_7^+ state in comparison to the 2_1^+ state is another indication of the mixed-symmetric nature of the 2_7^+ state, provided that the 3_2^- state is understood as the dominant fragment of the isoscalar octupole vibration of ^{202}Hg. Analogous $E1$-decay behaviors of fully-symmetric octupole excitations were observed in the case of ^{204}Hg [21], and of ^{92}Zr and ^{94}Mo [42]. ^{202}Hg exhibits an nearly unmixed, isolated $2_{1,\mathrm{ms}}^+$ state as was also observed earlier for ^{204}Hg [21] and ^{212}Po [20] in the vicinity of the doubly-magic nucleus ^{208}Pb. The $B(M1; 2_\mathrm{i}^+ \to 2_1^+)$ strength distributions observed in ^{202,204}Hg are compared in Fig. 4. In both Hg isotopes, a 2^+ level lies within an energy

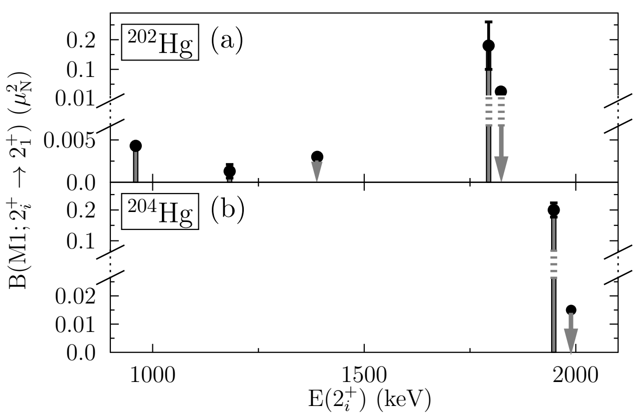

FIG. 4. $M1$ strength distributions $B(M1; 2_\mathrm{i}^+ \to 2_1^+)$ of ^{202}Hg (a) and ^{204}Hg (b). Upper limits are illustrated as arrow heads. The y-axes are divided into two parts with different scales.

range of 50 keV of the dominant $2_{1,\mathrm{ms}}^+$ fragment (cf. Fig. 4). It carries a small fraction of the total $M1$ strength to the 2_1^+ state. The upper limits for this $M1$ strength are $0.027\mu_\mathrm{N}^2$ in ^{202}Hg and $0.018\mu_\mathrm{N}^2$ in ^{204}Hg, respectively. For the quantification of the fragmentation of the $2_{1,\mathrm{ms}}^+$ states of ^{202,204}Hg, one determines the F-spin mixing matrix element $\mathrm{V_{mix}}$ in a two-state mixing scenario between the $2_{1,\mathrm{ms}}^+$ state and a close-lying 2^+ FSS [14]. Here, the $M1$ strength between FSSs has to be considered and is estimated as $B(M1; 2_2^+ \to 2_1^+) = 0.0043(8)\mu_\mathrm{N}^2$ for ^{202}Hg and is also applied to ^{204}Hg. Upper limits of the F-spin mixing matrix elements in Hg isotopes can then be determined: $\mathrm{V_{mix}}(^{202}\mathrm{Hg}) < 9(2)^{+3}_{-3}$ keV and $\mathrm{V_{mix}}(^{204}\mathrm{Hg}) < 11(1)^{+4}_{-5}$ keV. The F-spin mixing matrix elements determined for the $Z = 80$ isotopes are plotted in Fig. 5 as a function of the P factor [43] and compared to the literature values for the $N = 80$ isotones [14, 44]. The low F-spin mixing of $Z = 80$ isotopes and the $N = 80$ isotone ^{136}Ba $\mathrm{V_{mix}}(^{136}\mathrm{Ba}) < 10$ keV [14] demonstrates the preservation of the F-spin quantum number in the vicinity of shell closures in heavy nuclei and highlights the more strongly broken F-spin symmetry observed in ^{138}Ce $\mathrm{V_{mix}}(^{138}\mathrm{Ce}) = 44(3)\ ^{+3}_{-14}$ keV [14].

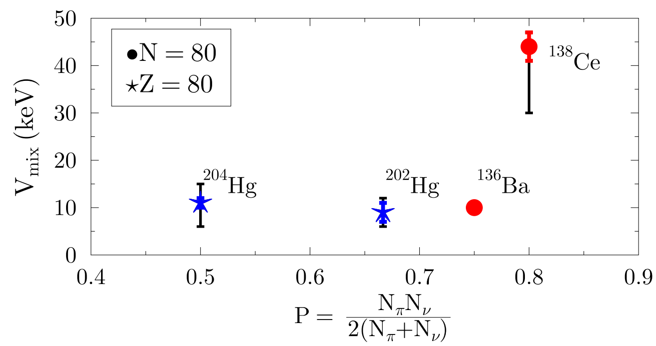

FIG. 5. (color online). F-spin mixing matrix elements $\mathrm{V_{mix}}$ of $N = 80$ isotones and $Z = 80$ isotopes as a function of P with statistical (color) and systematical error (black).

In conclusion, a projectile Coulomb excitation experiment was performed to identify the $2_{1,\mathrm{ms}}^+$ state of ^{202}Hg. In total, 39 transitions from excited states of ^{202}Hg, ten previously unknown, were observed and their branching ratios determined. These 39 transitions are assigned to 24 excited states, including a previously unknown one at 2681 keV. Information on 40 electromagnetic transition rates was deduced. In particular, the decay properties of the 2_7^+ state at 1794 keV were determined. Its comparatively large $M1$ strength justifies its assignment as the main fragment of the $2_{1,\mathrm{ms}}^+$ state of ^{202}Hg. This assumption is supported further by the measured absolute $E2$ transition strengths to the ground state and to the 2_1^+ state as well as by the R_{E1} ratio. Upper limits for F-spin mixing matrix elements $\mathrm{V_{mix}}$ in ^{202,204}Hg were determined. These indicate that F-spin is a well-conserved quantum number in these $Z = 80$ isotopes.

G.R. acknowledges the support from the Alexander von Humboldt foundation. N.P. and V.W. are supported by the DFG under Grant No. SFB 1245. This material is based upon work supported by the US Department of Energy, Office of Science, Office of Nuclear Physics, under Contract No. DE-AC02-06CH11357 and Grant Nos. DE-FG02-97ER41041(UNC) and DE-FG02-97ER41033(TUNL). This research used resources of ANL's ATLAS facility, which is a DOE Office of Science User Facility. This work was supported by BgNSF No. DN08/23, and by the BMBF under Grant Nos. 05P15(/18)RDFN1 and 05P15(/18)RDCIA.

[1] A. Bohr and B. Mottelson, *Nuclear structure, vol. II* (Benjamin, Reading, MA, 1975).
[2] A. Arima, T. Otsuka, F. Iachello, and I. Talmi, Phys. Lett. B **66**, 205 (1977).
[3] F. Iachello, Phys. Rev. Lett. **53**, 1427 (1984).
[4] F. Iachello and A. Arima, *The interacting boson model* (Cambridge University Press, 1987).
[5] W. D. Hamilton, A. Irbäck, and J. P. Elliott, Phys. Rev. Lett. **53**, 2469 (1984).
[6] N. Pietralla *et al.*, Phys. Rev. Lett. **83**, 1303 (1999).
[7] N. Pietralla *et al.*, Phys. Rev. Lett. **84**, 3775 (2000).
[8] U. Kneissl, N. Pietralla, and A. Zilges, J. Phys. G **32**, R217 (2006).
[9] N. Pietralla, P. von Brentano, and A. Lisetskiy, Prog. Part. and Nucl. Phys. **60**, 225 (2008).
[10] P. van Isacker, K. Heyde, J. Jolie, and A. Sevrin, Ann. Phys.(NY) **171**, 253 (1986).
[11] N. A. Smirnova, N. Pietralla, T. Mizusaki, and P. V. Isacker, Nucl. Phys. A **678**, 235 (2000).
[12] N. Pietralla *et al.*, Phys. Rev. C **64**, 031301 (2001).
[13] V. Werner *et al.*, Phys. Lett. B **550**, 140 (2002).
[14] G. Rainovski *et al.*, Phys. Rev. Lett. **96**, 122501 (2006).
[15] T. Ahn *et al.*, Phys. Lett. B **679**, 19 (2009).
[16] L. Coquard *et al.*, Phys. Rev. C **82**, 024317 (2010).
[17] K. A. Gladnishki *et al.*, Phys. Rev. C **82**, 037302 (2010).
[18] M. Danchev *et al.*, Phys. Rev. C **84**, 061306 (2011).
[19] T. Ahn *et al.*, Phys. Rev. C **86**, 014303 (2012).
[20] D. Kocheva *et al.*, Phys. Rev. C **93**, 011303 (2016).
[21] R. Stegmann *et al.*, Phys. Lett. B **770**, 77 (2017).
[22] I.-Y. Lee, Nucl. Phys. A **520**, c641 (1990).
[23] R. Gatenby, E. Kleppinger, and S. Yates, Nucl. Phys. A **492**, 45 (1989).
[24] A. Hogenbirk, H. Blok, and M. Harakeh, Nucl. Phys. A **524**, 251 (1991).
[25] P. Schuler *et al.*, Z.Phys. **A317**, 313 (1984).
[26] R. A. Moyer, Phys. Rev. C **5**, 1678 (1972).
[27] A. Bockisch, K. Bharuth-Ram, A. M. Kleinfeld, and K. P. Lieb, Z. Phys. **A291**, 245 (1979).
[28] Y. K. Agarwal *et al.*, Z. Phys. **A320**, 295 (1985).
[29] C. Lim, W. Catford, and R. Spear, Nucl. Phys. A **522**, 635 (1991).
[30] M. Lone, E. Earle, and G. Bartholomew, Nucl. Phys. A **243**, 413 (1975).
[31] A. Pakkanen, T. Komppa, and H. Helppi, Nucl. Phys. A **184**, 157 (1972).
[32] D. A. Craig and H. W. Taylor, J. Phys. G **10**, 1133 (1984).
[33] D. Breitig, R. F. Casten, W. R. Kane, G. W. Cole, and J. A. Cizewski, Phys. Rev. C **11**, 546 (1975).
[34] S. Zhu and F. G. Kondev, Nucl. Data Sheets **109**, 699 (2008).
[35] T. Kibèdi *et al.*, Nucl. Instrum. and Methods in Phys. Res. Sec. A **589**, 202 (2008).
[36] K. Alder, A. Winther, and J. L. Gammel, Physics Today **29**, 63 (1976).
[37] H. Ower, Dissertation, Johann Wolfgang Goethe-Universität Frankfurt am Main (1980).
[38] R. Spear *et al.*, Nucl. Phys. A **345**, 252 (1980).
[39] A. E. Stuchbery, P. F. Mantica, and A. N. Wilson, Phys. Rev. C **71**, 047302 (2005).
[40] W. Lewin, J. Bezemer, and C. V. Eijk, Nucl. Phys. **62**, 337 (1965).
[41] T. Czosnyka, D. Cline, and C. Y. Wu, *Coulomb Excitation Data Analysis Code* (Rochester, 2008).
[42] N. Pietralla *et al.*, Phys. Rev. C **68**, 031305 (2003).
[43] R. Casten and N. Zamfir, J. Phys. G **22**, 1521 (1996).
[44] N. Pietralla *et al.*, Phys. Rev. C **58**, 796 (1998).